

# Upconversion Luminescence Based Direct Hybridization Assay to Detect Subfemtomolar miR-20a DNA Analogue in Plasma

Saara Kuusinen,<sup>\*[a]</sup> Satu Lahtinen,<sup>[a]</sup> and Tero Soukka<sup>[a]</sup>

MicroRNAs (miRNAs) are promising biomarkers especially for early-stage cancer diagnostics, but the implementation of miRNA-based diagnostic tests is still hindered by the limitations of current analytical methods. The small size, low concentrations in biofluids and high sequence homology of miRNAs are challenges for assay development. Currently, most of the sensitive detection methods rely on enzymatic amplification steps, which complicate the analysis and can lead to biases in quantitation. Therefore, there is an increasing need to develop enzyme-free detection methods that are sensitive, specific and user-friendly. In this study, a simple direct hybridization assay

for the DNA analogue of miR-20a was developed. The assay is based on upconverting nanoparticle labels, which enable ultra-sensitive detection, and hairpin structured probes, which provide additional hybridization stability due to base stacking. The limit of detection was 0.73 fM with plasma recoveries between 76% and 111%, demonstrating that the assay could be used for direct detection of miRNAs from complex sample matrices without isolation of RNA. Due to the simplicity and the excellent sensitivity for an amplification-free method, the assay has a great potential for miRNA-based clinical applications.

## Introduction

Micro-RNAs (miRNA) are short non-coding RNA molecules that have an important role in the regulation of the gene expression at the post-transcriptional level.<sup>[1]</sup> They are present in several tissues and body fluids, including blood, urine, saliva and cerebrospinal fluid.<sup>[2]</sup> A wide range of studies have demonstrated correlation between miRNA expression levels and various diseases, such as cancers, cardiovascular diseases and infectious diseases, and there are numerous reviews about the topic.<sup>[3]</sup> As miRNAs are involved in the development of diseases, changes in their concentrations occur already at early disease stage, making miRNAs promising biomarkers for early diagnostics.<sup>[4]</sup> However, due to their small size, high sequence homology and low concentrations in body fluids (atto-femtomolar range in blood),<sup>[5]</sup> developing assays that are sensitive enough to detect changes in specific miRNA concentrations and still simple enough for routine diagnostics is challenging.

Conventional miRNA detection methods, including quantitative reverse transcription polymerase chain reaction (RT-qPCR), microarray, next generation sequencing and Northern blotting, each have their limitations concerning routine diag-

nostic use.<sup>[6]</sup> Development of novel detection technologies is accelerating, but the most sensitive strategies usually include target amplification either by PCR or isothermal amplification.<sup>[7]</sup> These methods are laborious and time-consuming and require specialized laboratory facilities and careful purification of RNA to remove enzyme inhibitors in the sample.<sup>[8]</sup> Both, purification and amplification of miRNAs introduce sources of errors and sequence-dependent biases to the workflow, generating a serious obstacle for method standardization.<sup>[6a,9]</sup>

A wide range of target amplification-free methods for miRNA detection have been developed, but the most sensitive methods utilize enzyme cascade for signal amplification step. Bruch *et al.* (2019) developed a CRISPR/Cas13a-powered electrochemical microfluidic biosensor for detection of miR-20a, which was able to detect picomolar concentrations without target amplification.<sup>[10]</sup> Sha *et al.* (2021) improved the sensitivity by approximately 1000-fold by developing a cascade CRISPR/Cas system for detection of miR-17.<sup>[11]</sup> However, due to the use of enzymes, these assays are not suitable for direct detection of miRNAs without RNA isolation from the sample. The sensitivities of enzyme-free assays are typically at picomolar level.<sup>[12]</sup>

The short length of miRNAs is a significant challenge for the design of probes and primers for their detection. The hybridization of short sequences can be stabilized by utilizing base stacking, which refers to the interactions between adjacent bases, and it stabilizes the probe hybridization at nick sites.<sup>[13]</sup> The stacking effect contributes to the overall duplex stability even more than the hydrogen bonds in the base pairing.<sup>[14]</sup> Base stacking has been utilized in several applications to stabilize hybridization of short sequences, including PCR, biosensing and sequencing.<sup>[7f,11,12c,15]</sup> Qiu *et al.* (2015) employed base stacking in Förster resonance energy transfer (FRET) based quantum dot biosensor for miRNAs. The assay was based on an

[a] S. Kuusinen, S. Lahtinen, T. Soukka  
 Department of Life Technologies, Faculty of Technology, University of Turku,  
 Kiinamyllynkatu 10, 20520 Turku, Finland  
 E-mail: saevku@utu.fi

Supporting information for this article is available on the WWW under  
<https://doi.org/10.1002/anse.202400005>

© 2024 The Authors. Analysis & Sensing published by Wiley-VCH GmbH. This is an open access article under the terms of the Creative Commons Attribution Non-Commercial License, which permits use, distribution and reproduction in any medium, provided the original work is properly cited and is not used for commercial purposes.

acceptor probe with an overhang that could only hybridize with donor-DNA in the presence of target RNA, which stabilized the hybridization by base stacking. The sensor was able to detect three miRNAs in a simple mix-and-measure format with a sensitivity of 2–10 nM.<sup>[16]</sup> The sensitivity was later improved by more than 20-fold by using upconverting nanoparticles (UCNPs) as donors instead of quantum dots.<sup>[12c]</sup>

UCNPs have attracted wide interest as reporters in bio-analytical assays due to their exceptional detectability. They can convert low-energy excitation into higher-energy emission upon sequential absorption of multiple photons, thus enabling complete spectral elimination of autofluorescence background.<sup>[17]</sup> Even though the quantum yield of UCNPs is typically low, the total absence of autofluorescence at emission wavelengths enables the detection of trace amounts of UCNPs.<sup>[18]</sup> Therefore, UCNPs have a great potential to significantly improve the sensitivity of bioanalytical assays.<sup>[12c,19]</sup> Tsang *et al.* (2016) applied UCNPs in an amplification free assay to detect Ebola virus oligonucleotides. The assay was capable of detecting femtomolar concentrations, which was comparable to the sensitivity of typical RT-qPCR methods.<sup>[20]</sup> Mendez-Gonzalez *et al.* (2018) developed an upconversion based heterogenous hybridization assay for detection of miR-195 on streptavidin coated microtiter plates. They utilized target sequence dependent photoligation to form covalent UCNP-biotin conjugates in a presence of miR-195, allowing for efficient elimination of nonspecific binding by stringent washing. The assay had a limit of detection (LoD) of 21 fM.<sup>[21]</sup> In addition to the exceptional detection sensitivity, UCNPs also allow for simultaneous detection of multiple analytes by either spatial or spectral multiplexing,<sup>[22]</sup> which is beneficial in miRNA-based diagnostic applications.

In this article, we present a simple heterogenous hybridization assay for detection of subfemtomolar concentrations of miR-20a DNA analogue by using UCNPs as reporters. The sensitivity of the assay was improved by exploiting DNA stacking obtained by hairpin-structured capture and tracer probes. The assay was compared with a similar assay utilizing linear probes. The developed assay is enzyme-free and therefore suitable for detection of miRNAs directly from complex sample matrices without RNA purification. It is also compatible with conventional microtiter plate assay protocols and can be easily adapted for the detection of other miRNAs.

## Results and Discussion

### The Effect of Probe Structure and NaCl Concentration to Probe Hybridization

The DNA sequences used in this work are presented in Table 1. Synthetic DNA oligonucleotide corresponding to miRNA sequence miR-20a was used as a model target. Poly(acrylic acid) coated NaYF<sub>4</sub>:Yb<sup>3+</sup>, Er<sup>3+</sup> UCNPs covalently functionalized with either linear or hairpin-structured DNA tracer probes were used as labels in the heterogeneous hybridization assays. The assays were carried out by first mixing the calibrators or samples with

**Table 1.** Oligonucleotide sequences and modifications.

Name	Sequence (5'–3') <sup>[a]</sup>	Modification
<b>Probes</b>		
hairpin capture	TAT AAG CAC TTT AGG AGA CGT CCA TA* GTA GGA CGT CTC C	* = biotin dT
linear capture	TAT AAG CAC TTT AGG AGA CGT CCA TAT	3'-biotin-TEG
hairpin tracer	CTC GTG ACC GTA G*T ACC GGT CAC GAG CTA CCT GCA C	* = amino C6 dT
linear tracer	TTA CCG GTC ACG AGC TAC CTG CAC	5'-aminolink-C6
<b>Targets</b>		
DNA-miR-20a	TAA AGT GCT TAT AGT GCA GGT AG	none
DNA-miR-20b (non-complementary, 2 mismatches)	<u>C</u> AA AGT GCT <u>C</u> AT AGT GCA GGT AG	none
1 mismatch	TAA AGT GCT TAT A <u>I</u> T GCA GGT AG	none
3 mismatches	<u>C</u> AA AGT GCT <u>C</u> AT A <u>I</u> T GCA GGT AG	none
long	C <u>I</u> TAA AGT GCT TAT AGT GCA GGT AGA <u>G</u>	none
short	A AGT GCT TAT AGT GCA GGT	none

[a] Underlined parts are mismatches. [\*] Stands for internal modifications.

UCNP labels diluted into assay buffer, using 80:20 volume ratio if not otherwise stated. After 2 h 45 min incubation, the hybridization reaction mixtures were pipetted to streptavidin microtiter wells coated with either linear or hairpin-structured biotin modified DNA capture probes and incubated for 1 h. The wells were washed and the upconversion luminescence (UCL) signals at 540 nm were measured from the bottoms of the dry wells upon 980 nm laser excitation.

The assay employing hairpin-structured DNA probes was compared with a similar assay employing linear DNA probes. The hybridization of both of the probes in both assays is illustrated in Figure 1. The effect of probe structure to the hybridization efficiency and sensitivity were studied by performing both assays in NaCl concentrations from 0.15 M to 0.84 M. The hybridization reactions contained 40% proportion of 5 pM calibrator and 60% of UCNPs diluted into assay buffer supplemented with NaCl and KF, resulting in 0.15, 0.32, 0.5, 0.67 and 0.84 M NaCl and 1 mM KF in the final reaction mixture. With hairpin-structured probes, the UCL signals were higher than with linear probes in all NaCl concentrations, suggesting that the base stacking caused by the hairpin structure significantly stabilizes the hybridization (Figure 2A). The difference of the probe types in hybridization efficiency decreased when the NaCl concentration was increased, as the increasing ionic strength stabilizes the hybridization. However, the analyte-dependent UCL remained approximately twice as high with

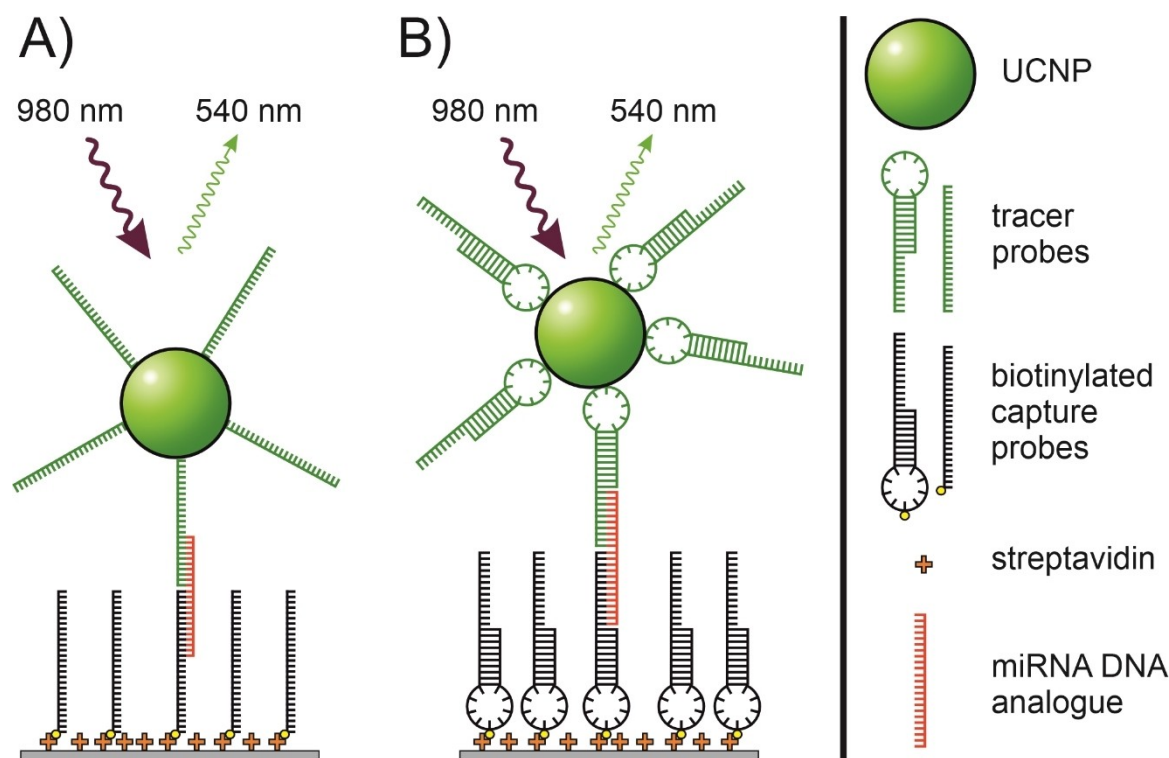


Figure 1. Schematic illustration of the hybridization assay using A) linear and B) hairpin structured probes.

hairpin-structured probes compared to the linear probes. Even at 0.15 M NaCl, the UCL with hairpin-structured probes was almost as high as the maximum UCL with the linear probes. Interestingly, the UCNPs conjugated with linear tracer probes had 2–16 times higher nonspecific binding than the UCNPs conjugated with hairpin-structured probes (Figure 2B). Increasing the NaCl concentration in the hybridization reaction decreased the nonspecific binding, which is most likely due to the prevention of electrostatic interactions between the UCNP conjugates and the capture surface.

The hybridization stability of the linear and hairpin-structured probes was also evaluated in solution by melting curve analysis, and the hairpin-structured probes showed stronger hybridization with the target DNA than linear probes (Figure S2).

### Assay Performance

Each calibrator of the standard curve was analyzed in three replicates, except for the blank calibrator in eight replicates. The standard curves for the hybridization assays with hairpin-structured and linear capture and tracer probes are presented in Figure 3. Logistic regression of Origin 2016 was used for fitting the standard curves. The NaCl concentration in hybridization reactions was 0.6 M. The limit of detection (LoD) of the assay was determined according to the IUPAC guidelines as concentration corresponding to the signal response equivalent to  $3\times$  standard deviation of the zero calibrator. The LoD was 0.73 fM for hairpin-structured probes and 13 fM for linear

probes, corresponding to approximately 52 000 and 960 000 copies of DNA-miR-20a in the reaction volume per well, respectively. The sensitivity of the assay utilizing hairpin-structured probes was excellent for an assay without any target or signal amplification. Cui *et al.* (2021) developed an electrochemical assay for miR-21 based on CRISPR/Cas13a with a LoD of 2.6 fM. The assay had excellent recoveries when the target was spiked into 10-fold diluted serum.<sup>[23]</sup> However, if the sample needs to be diluted 10-fold to prevent matrix-related interferences, the miRNA concentration in the actual serum sample would need to be 10 times higher to be detectable, which was not taken into account in the LoD. Špringer *et al.* (2021) achieved a sensitivity of 350 aM, which is approximately 2 times lower than ours, with a surface plasmon resonance-based nanoparticle release assay for miR-125b, but they used ten times larger sample volume, and thus, the lowest detectable amount of molecules was actually higher.<sup>[24]</sup>

The analyte-dependent specific signals were about 30% higher with hairpin-structured probes compared to the corresponding linear probes. The difference in the sensitivities achieved with hairpin-structured and linear probes was mostly caused by the approximately 10-fold difference in nonspecific binding of the UCNP conjugates. Nonspecific binding was further studied by cross-testing all combinations of the hairpin-structured and linear capture and tracer probes. The low nonspecific binding was associated with the UCNPs conjugated with hairpin-structured DNA probes, whereas the type of the capture probes had neglectable effect on the nonspecific binding (Figure S6).

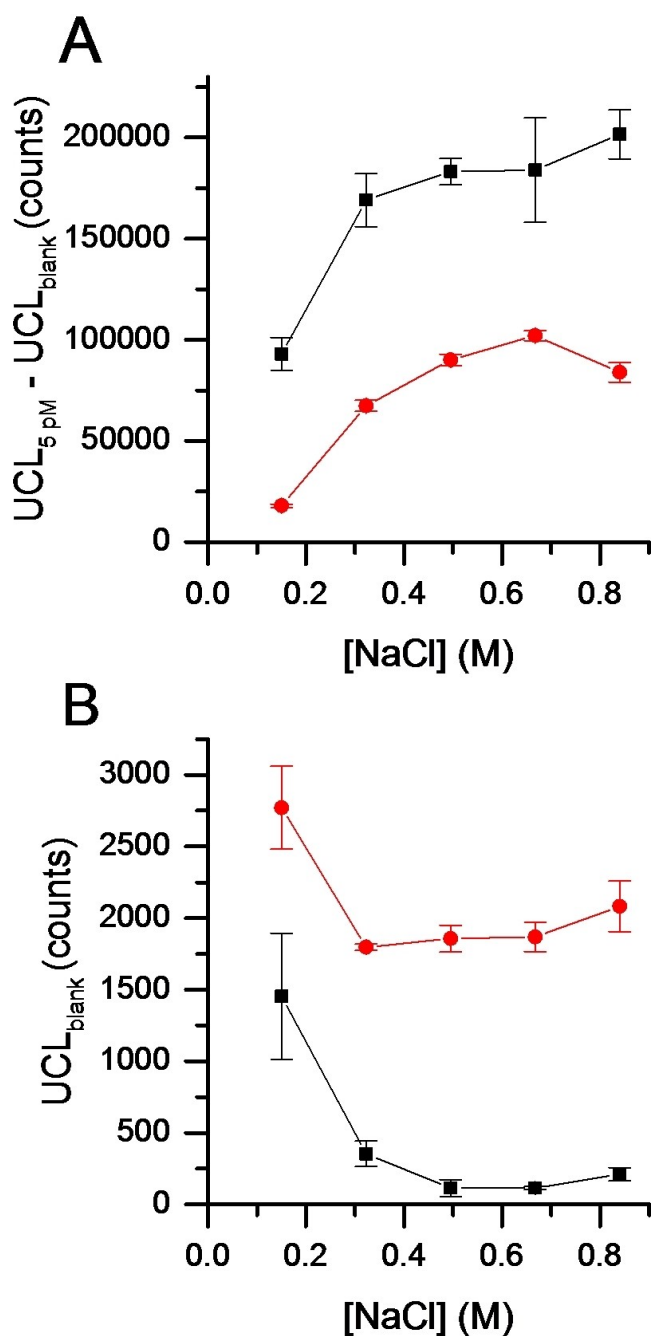


**Figure 2.** The effect of NaCl concentration on A) hybridization efficiency with 5 pM calibrator and B) nonspecific binding of UCNPs using hairpin structured (black, squares) and corresponding linear (red, circles) capture and tracer probes. The sample proportion of the total reaction volume was 40%, and concentrations of capture probes and UCNPs conjugates were kept constant in both assays. The error bars represent the standard deviation of three replicates.

In the standard curves (Figure 3), the difference in specific signals between the probe types was smaller than in the comparison of the hybridization efficiency in varying NaCl concentration (Figure 2A). The results are not directly comparable, because in the standard curves, the proportion of the sample of the total reaction volume was 80%, whereas in the comparison of varying NaCl concentration, the sample propor-

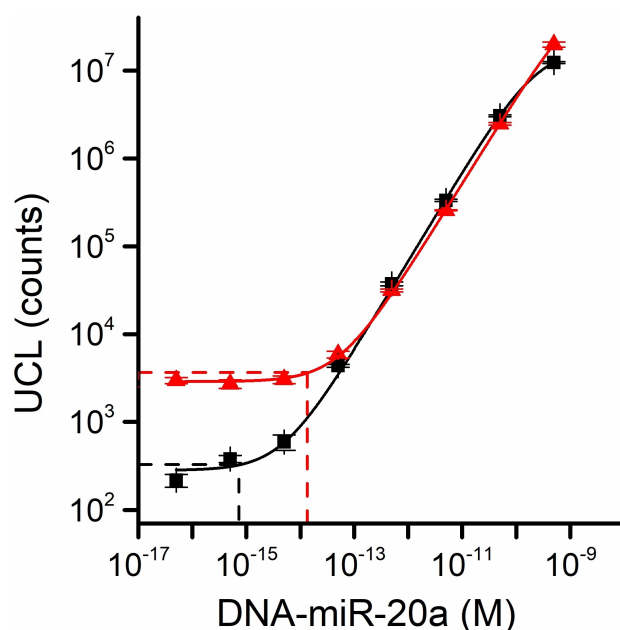


**Figure 3.** Standard curves using hairpin structured (black, squares) and corresponding linear (red, triangles), capture and tracer probes and 80% sample proportion of the total reaction volume. Dashed lines show the limits of detection (LoD), which were 0.73 fM for hairpin structured probes and 13 fM for linear probes and the error bars represent the standard deviation of three replicates of the calibrators.

tion was only 40%. The calibrators were prepared in 50 mM Tris-HCl, pH 7.75, 7.5% BSA, and it is possible that the high protein concentration has a different effect on the signal levels achieved with hairpin-structured and linear probes.

### Recovery Testing

In order to demonstrate the feasibility of the assay for direct detection of analyte in complex biological samples, plasma recoveries were determined. The plasma recovery percentages from 0.05, 0.5, 5 and 50 pM DNA-miR-20a spiked into EDTA plasma pool were 111%, 93%, 89% and 76%, respectively. EDTA plasma was chosen as a sample matrix, because EDTA inhibits nuclease activity, which is especially critical when working with RNA targets. However, UCNPs conjugates have a tendency to form aggregates in complex biological matrices decreasing their reactivity with the analyte, which can lead to lower signal response in biological matrices.<sup>[25]</sup> Juntunen *et al.* (2016) demonstrated in lateral flow immunoassay, that UCNPs-antibody conjugates were more likely to aggregate in EDTA plasma than other blood matrices.<sup>[25b]</sup> However, our results imply that major aggregation does not happen to UCNPs-DNA conjugates in our assay conditions, as the standard deviations between the three replicates of spiked plasma samples were between 1–8% (data not shown). It is possible, that the recoveries could be improved by increasing the concentration of UCNPs conjugates in the hybridization reactions. While there is still room for improvement, the results indicate that the assay

can be used for sensitive detection of miRNA directly from plasma without isolation of RNA.

### Cross-Reactivity

The ability of the assay to discriminate between DNA sequences corresponding to two highly homologous miRNAs was demonstrated by analyzing calibrators containing various combinations of DNA-miR-20a and DNA-miR-20b. The assay had 5% cross-reactivity with DNA-miR-20b (Figure 4a). DNA-miR-20b has only two mismatched bases compared to DNA-miR-20a, which are both located at the sequence that is complementary to the capture probe. One of the mismatches is at the 5' end of the target, which is right next to the nick between the target and the capture probe. Therefore, the mismatch should affect on the stabilization of the nick by base stacking. The other mismatch is three bases from the nick between the capture and tracer probes.

Cross-reactivity was also studied by testing calibrators containing 5 pM of DNA oligonucleotides with small variations to the sequence of the complementary target. The variations included 1, 2 (miR-20b) and 3 mismatches, 2 base overhangs at both ends of the target sequence and a sequence that is 2 bases shorter at both ends compared to DNA-miR-20a. Of these variations, the sequence with 2 base overhangs had highest cross-reactivity, 34% of the signal of the complementary target. Since this sequence contains the complete sequence of the complementary target, the 66% loss in signal is caused by the steric hindrance and loss of stabilization effect of the base stacking due to the overhangs. The sequence with only one mismatch resulted in 11% cross-reactivity, and the rest of the variations in 0–5% cross-reactivity. Cross-reactivity could probably be decreased by further optimization of the assay conditions, for example by decreasing the ionic strength of the assay buffer.

### Conclusions

An amplification-free method for ultrasensitive detection of short nucleic acid targets was developed. The sensitivity is based on highly detectable UCNP labels and the use of hairpin structured probes, which increase the hybridization stability of the probes and the short target DNA via base stacking. The developed assay demonstrates the great potential of UCNP for ultra-sensitive detection of biomarkers directly from complex sample materials. The assay is highly promising for miRNA-based diagnostic applications, because it is simple to perform and compatible with conventional microtiter plate-based assay protocols. The concentration of miR-20a in blood has been reported to be at picomolar level, which is more than 3 orders of magnitude higher than the LoD of our assay.<sup>[26]</sup> By changing the probe sequences, the assay could also be easily modified for detection of other miRNA targets. The technique is also suitable for simultaneous detection of multiple miRNAs by spatial and spectral multiplexing, like the serological array-in-

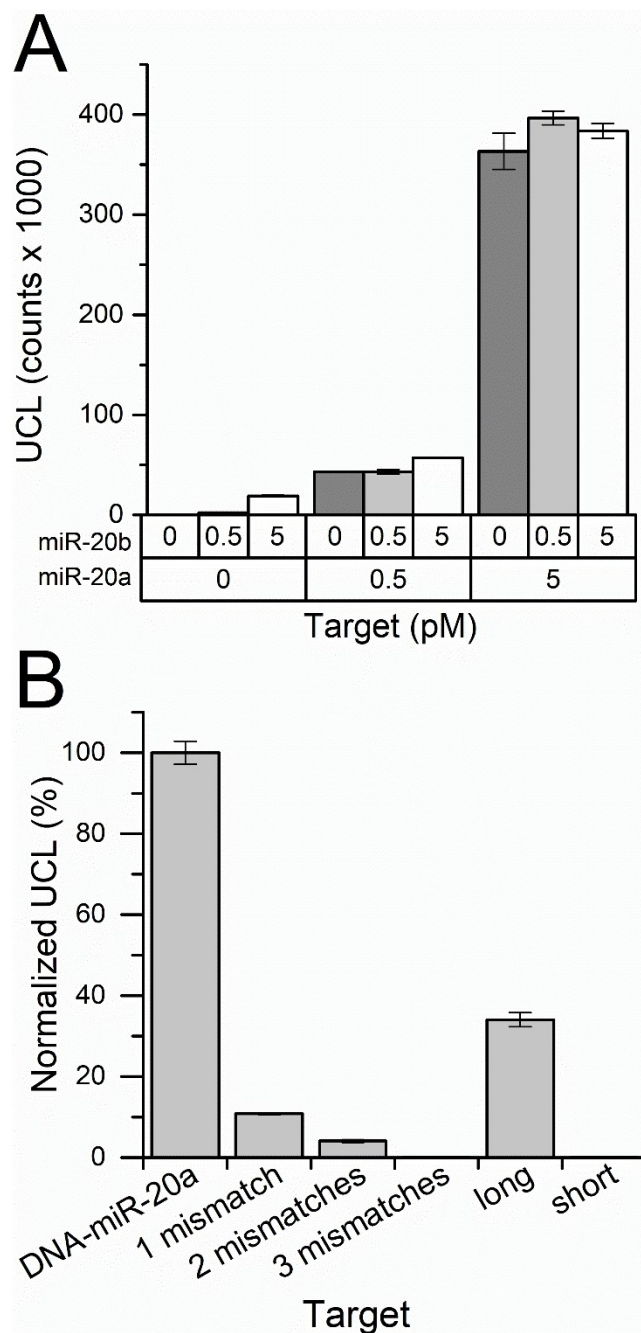


**Figure 4.** Cross-reactivity of the assay with highly homologous sequences. A) Calibrators containing various combinations of complementary (DNA-miR-20a) and non-complementary (DNA-miR-20b) target were analyzed with the assay using hairpin structured probes. The heights of the bars represent the UCL signals in calibrators containing 0, 0.5 and 5 pM of DNA-miR-20a mixed with 0, 0.5 and 5 pM of DNA-miR-20b. B) Calibrators containing 5 pM of DNA with small variations to the target sequence were analyzed with the assay using hairpin structured probes. “Long” means a sequence with 2 base overhangs at both ends and “short” means sequence that is two bases shorter at both ends compared to the complementary target DNA-miR-20a. The exact sequences are presented in Table 1. The error bars show the standard deviation of three replicate measurements.

well developed by Kale et al. (2016).<sup>[22b]</sup> The assay development and performance testing were done by using synthetic DNA oligonucleotide corresponding to the sequence of miR-20a as

target. No actual miRNA detection was tested, but since thermal stability of hybridization between DNA-DNA duplexes has been reported to be close to that of DNA-RNA heteroduplexes, similar assay performance can be expected for detection of miRNA.<sup>[27]</sup>

## Experimental Section

### Synthesis and Surface Modification of UCNP-DNA Conjugates

NaYF<sub>4</sub>:Yb<sup>3+</sup>, Er<sup>3+</sup> UCNPs (17% Yb<sup>3+</sup>, 3% Er<sup>3+</sup>) were synthesized in organic oils as described previously.<sup>[28]</sup> The size of the oleic acid-capped UCNPs was measured with transmission electron microscopy (TEM) imaging, which is described in Supporting Information (SI). The UCNPs were coated with poly(acrylic acid) (PAA, MW 2000, Sigma-Aldrich, Saint Louis, Missouri, USA) as described previously<sup>[19a]</sup> and conjugated with amino modified tracer probes using carbodiimide crosslinking. Before conjugation, the probes were dissolved in conjugation buffer (20 mM 2-(N-morpholino) ethanesulfonic acid (MES), pH 6.5) in a concentration of 0.167 mM, heated to 95 °C for 5 min to denature any possible dimers, and let cool at room temperature. PAA-coated UCNPs were transferred to conjugation buffer by centrifugation at 20 237 g for 10 min and sonicated with a VialTweeter sonicator (10 cycles, 0.5 s with 100% amplitude, Hielscher Ultrasonics GmbH, Teltow, Germany). The conjugation was done in 250 µL of conjugation buffer containing 20 mM N-(3-dimethylaminopropyl)-N'-ethylcarbodiimide (EDC, Sigma-Aldrich), 30 mM N-hydroxysulfosuccinimide (sulfo-NHS, TCI Chemicals, Tokyo, Japan) and 20 nmol of tracer probes per 2.5 mg UCNPs. The reaction was incubated for 2.5 h under slow rotation, after which, the surface of the UCNPs was blocked by adding 50 mM 2-amino-N,N-dimethylacetamide (ADMA) and slowly rotating the tube for 30 min. The conjugates were washed by centrifugation (20 237 g, 10 min) four times with 10 mM Tris-HCl (pH 8.5) containing 0.1% (w/v) Tween 20. In the first two washes, the conjugate suspension was heated to 95 °C for 5 min before centrifugation to denature possible probe dimers. Finally, the UCNP conjugates were suspended into 250 µL of storage buffer (5 mM Tris-HCl, pH 8.5, 0.2% Tween-85, 50 µM EDTA, 0.05% Na<sub>3</sub>) and stored at +4 °C.

### Hybridization Assay

Assay buffer, wash buffer and streptavidin coated 96-well microtiter plates (KaiSA-Lockwell White) were purchased from Uniogen (Turku, Finland). The optimization of UCNP concentration and incubation time are described in detail in the SI. Calibrators were prepared by diluting target DNA oligonucleotides into 50 mM Tris, pH 7.75, 150 mM NaCl, 7.5% (w/v) bovine serum albumin (Bioreba, Reinach, Switzerland). UCNP conjugates were diluted to a final concentration of 5 µg/mL into hybridization buffer (assay buffer supplemented with 2.25 M NaCl and 5 mM KF) and bath sonicated for 3 min just before starting the assay. Calibrators or samples were mixed with diluted UCNP conjugates using 80:20 volume ratio and the hybridization reactions were incubated at room temperature under 1200 rpm orbital shaking for 2 h 45 min.

Capture probes with biotin modification were diluted to a final concentration of 50 nM into assay buffer supplemented with 5% EtOH. The dilution was heated to 80 °C under 1 000 rpm shaking for 5 min to denature probe dimers and let cool at room temperature. Streptavidin coated microtiter plate was prewashed and 25 µL of capture probe solution was added to each well. After 30 min incubation, the wells were washed once and 150 µL of pre-incubated hybridization reaction mixture was added to each well.

The plate was incubated under slow shaking for 60 min and washed four times with wash buffer supplemented with 0.3 M NaCl, 0.1% (w/v) Tween 20 and 1 mM KF. The UCL signals at 540 nm were measured from the bottoms of the dry wells by using modified Plate Chameleon fluorometer (Hidex Oy, Turku, Finland) equipped with a 980 nm laser.<sup>[29]</sup> A 3×3 point raster was measured from each well, and the average of the 9 points was calculated.

### Plasma Pool

The plasma recoveries were determined by spiking DNA-miR-20a into EDTA plasma pool. No ethical approval was sought as no individual samples were analyzed and the obtained plasma pool was only for the purpose of blank matrix to be spiked with synthetic DNA oligonucleotides to examine the analyte recovery. Blood for the plasma pool was collected from 10 apparently healthy volunteers with informed consent in compliance with the declaration of Helsinki. Blood was collected in EDTA vacuum tubes (Vacuette 9 mL, Greiner Bio-One, Kremsmünster, Austria), the samples were anonymized and plasma was separated by centrifugation according to the manufacturer's instructions. Plasma samples were pooled and the pool aliquots were spiked with 0, 0.05, 0.5, 5 and 50 pM DNA-miR-20a to be analyzed with the hybridization assay.

## Supporting Information

Measurement of the size of the oleic acid-capped UCNPs, melting analysis of the probe hybridization, optimization of the hybridization assay and crosswise testing of nonspecific binding with all probe combinations (PDF).

## Acknowledgements

The work was supported by a grant from Instrumentarium Science Foundation. The authors thank Jaana Rosenberg at University of Turku for synthesizing and Kirsti Raiko for TEM-imaging the UCNPs. TEM images were taken in the Laboratory of Electron Microscopy at the University of Turku.

## Conflict of Interests

The authors declare no conflict of interest.

## Data Availability Statement

The data that support the findings of this study are available from the corresponding author upon reasonable request.

**Keywords:** base stacking · miRNA diagnostics · nanoparticles · oligonucleotides · upconversion

[1] D. P. Bartel, *Cell* **2004**, *116*, 281–297.

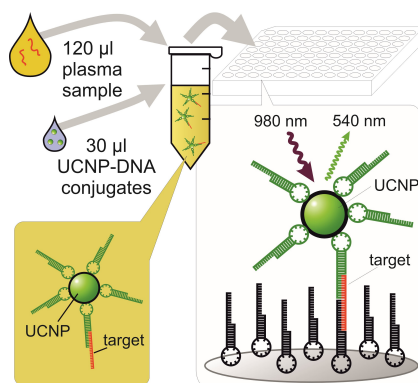
[2] J. A. Weber, D. H. Baxter, S. Zhang, D. Y. Huang, K. How Huang, M. Jen Lee, D. J. Galas, K. Wang, *Clinical Chemistry* **2010**, *56*, 1733–1741.

- [3] a) S. Lin, R. I. Gregory, *Nat. Rev. Cancer* **2015**, *15*, 321–333; b) H. Wang, R. Peng, J. Wang, Z. Qin, L. Xue, *Clinical epigenetics* **2018**, *10*, 1–10; c) M. V. Iorio, C. M. Croce, *EMBO molecular medicine* **2012**, *4*, 143–159; d) J. Wang, J. Chen, S. Sen, *J. Cell. Physiol.* **2016**, *231*, 25–30; e) C. N. Correia, N. C. Nalpas, K. E. McLoughlin, J. A. Browne, S. V. Gordon, D. E. MacHugh, R. G. Shaughnessy, *Front. Immunol.* **2017**, *8*, 118.
- [4] a) H. Zhang, F. Mao, T. Shen, Q. Luo, Z. Ding, L. Qian, J. Huang, *Oncology letters* **2017**, *13*, 669–676; b) Q. Geng, T. Fan, B. Zhang, W. Wang, Y. Xu, H. Hu, *Respiratory research* **2014**, *15*, 1–9; c) A. Arab, M. Karimipoor, S. Irani, A. Kiani, S. Zeinali, E. Tafsiiri, K. Sheikhy, *Cancer Genetics* **2017**, *216*, 150–158.
- [5] P. S. Mitchell, R. K. Parkin, E. M. Kroh, B. R. Fritz, S. K. Wyman, E. L. Pogosova-Agadjanyan, A. Peterson, J. Noteboom, K. C. O'Briant, A. Allen, *Proc. Natl. Acad. Sci. USA* **2008**, *105*, 10513–10518.
- [6] a) L. Valihrach, P. Androvic, M. Kubista, *Mol. Aspects Med.* **2020**, *72*, 100825; b) V. P. Dave, T. A. Ngo, A.-K. Pernestig, D. Tilevik, K. Kant, T. Nguyen, A. Wolff, D. D. Bang, *Lab. Invest.* **2019**, *99*, 452–469.
- [7] a) G. Zhang, L. Zhang, J. Tong, X. Zhao, J. Ren, *Microchem. J.* **2020**, *158*, 105239; b) J. Song, Y. Ju, S. Kim, H. Kim, H. G. Park, *Chem. Commun.* **2022**, *58*, 6518–6521; c) P. Mestdagh, N. Hartmann, L. Baeriswyl, D. Andreasen, N. Bernard, C. Chen, D. Cheo, P. D'andrade, M. DeMayo, L. Dennis, *Nat. Methods* **2014**, *11*, 809–815; d) P. Androvic, L. Valihrach, J. Elling, R. Sjoback, M. Kubista, *Nucleic Acids Res.* **2017**, *45*, e144–e144; e) H. Jia, Z. Li, C. Liu, Y. Cheng, *Angew. Chem. Int. Ed.* **2010**, *49*, 5498–5501; f) C. Chen, D. A. Ridzon, A. J. Broomer, Z. Zhou, D. H. Lee, J. T. Nguyen, M. Barbisin, N. L. Xu, V. R. Mahuvakar, M. R. Andersen, *Nucleic Acids Res.* **2005**, *33*, e179–e179.
- [8] D.-J. Kim, S. Linnstaedt, J. Palma, J. C. Park, E. Ntrivalas, J. Y. Kwak-Kim, A. Gilman-Sachs, K. Beaman, M. L. Hastings, J. N. Martin, *The Journal of Molecular Diagnostics* **2012**, *14*, 71–80.
- [9] a) D. W. Wegman, S. N. Krylov, *TrAC Trends Anal. Chem.* **2013**, *44*, 121–130; b) V. Klotten, M. H. Neumann, F. Di Pasquale, M. Sprenger-Haussels, J. M. Shaffer, M. Schlumpberger, A. Herdean, F. Betsou, W. Ammerlaan, T. af Hällström, *Clinical Chemistry* **2019**, *65*, 1132–1140.
- [10] R. Bruch, J. Baaske, C. Chatelle, M. Meirich, S. Madlener, W. Weber, C. Dincer, G. A. Urban, *Adv. Mater.* **2019**, *31*, 1905311.
- [11] Y. Sha, R. Huang, M. Huang, H. Yue, Y. Shan, J. Hu, D. Xing, *Chem. Commun.* **2021**, *57*, 247–250.
- [12] a) J. Pu, M. Liu, H. Li, Z. Liao, W. Zhao, S. Wang, Y. Zhang, R. Yu, *Talanta* **2021**, *230*, 122158; b) X. Zhao, S. Wang, R. Zou, C. Chen, C. Cai, *Microchim. Acta* **2021**, *188*, 1–8; c) L. Francés-Soriano, N. Estebanez, J. Pérez-Prieto, N. Hildebrandt, *Adv. Funct. Mater.* **2022**, *32*, 2201541; d) S. Zhao, S. Yang, H. Xu, X. Tang, H. Wang, L. Yu, X. Qiu, Y. Wang, M. Gao, K. Chang, *Anal. Chim. Acta* **2022**, *1191*, 339282.
- [13] E. Protozanova, P. Yakovchuk, M. D. Frank-Kamenetskii, *J. Mol. Biol.* **2004**, *342*, 775–785.
- [14] P. Yakovchuk, E. Protozanova, M. D. Frank-Kamenetskii, *Nucleic Acids Res.* **2006**, *34*, 564–574.
- [15] C.-Y. Yu, B.-C. Yin, B.-C. Ye, *Chem. Commun.* **2013**, *49*, 8247–8249.
- [16] X. Qiu, N. Hildebrandt, *ACS Nano* **2015**, *9*, 8449–8457.
- [17] F. Auzel, *Chem. Rev.* **2004**, *104*, 139–174.
- [18] a) J.-C. Boyer, F. C. Van Veggel, *Nanoscale* **2010**, *2*, 1417–1419; b) C. T. Xu, Q. Zhan, H. Liu, G. Somesfalean, J. Qian, S. He, S. Andersson-Engels, *Laser Photonics Rev.* **2013**, *7*, 663–697.
- [19] a) K. Raiko, A. Lyytikäinen, M. Ekman, A. Nokelainen, S. Lahtinen, T. Soukka, B. I. Martiskainen, E. Juntunen, T. Salminen, K. Vuorenperä, S. Bayoumy, T. Vuorinen, N. Khanna, K. Pettersson, G. Batra, S. M. Talha, H. H. Gorris, *Anal. Chem.* **2017**, *89*, 11825–11830.
- [20] M.-K. Tsang, W. Ye, G. Wang, J. Li, M. Yang, J. Hao, *ACS Nano* **2016**, *10*, 598–605.
- [21] D. Mendez-Gonzalez, S. Lahtinen, M. Laurenti, E. López-Cabarcos, J. Rubio-Retama, T. Soukka, *Anal. Chem.* **2018**, *90*, 13385–13392.
- [22] a) F. Van De Rijke, H. Zijlmans, S. Li, T. Vail, A. K. Raap, R. S. Niedbala, H. J. Tanke, *Nat. Biotechnol.* **2001**, *19*, 273–276; b) V. Kale, H. Pääkkilä, J. Vainio, A. Ahomaa, N. Sirkka, A. Lyytikäinen, S. M. Talha, A. Kutsaya, M. Waris, *J. J. J. Anal. Chem.* **2016**, *88*, 4470–4477.
- [23] Y. Cui, S. Fan, Z. Yuan, M. Song, J. Hu, D. Qian, D. Zhen, J. Li, B. Zhu, *Talanta* **2021**, *224*, 121878.
- [24] T. Špringer, Z. Krejčík, J. Homola, *Biosens. Bioelectron.* **2021**, *194*, 113613.
- [25] a) S. Lahtinen, S. Krause, R. Arppe, T. Soukka, T. Vosch, *Chem. Eur. J.* **2018**, *24*, 9229–9233; b) E. Juntunen, R. Arppe, L. Kalliomäki, T. Salminen, S. M. Talha, T. Myyryläinen, T. Soukka, K. Pettersson, *Anal. Biochem.* **2016**, *492*, 13–20; c) S. J. Budijono, J. Shan, N. Yao, Y. Miura, T. Hoye, R. H. Austin, Y. Ju, R. K. Prud'homme, *Chem. Mater.* **2010**, *22*, 311–318.
- [26] X. Zhou, W. Zhu, H. Li, W. Wen, W. Cheng, F. Wang, Y. Wu, L. Qi, Y. Fan, Y. Chen, Y. Ding, J. Xu, J. Qian, Z. Huang, T. Wang, D. Zhu, Y. Shu, P. Liu, *Sci. Rep.* **2015**, *5*, 11251.
- [27] B. I. Kankia, L. A. Marky, *J. Phys. Chem. B* **1999**, *103*, 8759–8767.
- [28] E. Palo, M. Tuomisto, I. Hyppänen, H. C. Swart, J. Hölsä, T. Soukka, M. Lastusaari, *J. Lumin.* **2017**, *185*, 125–131.
- [29] T. Soukka, K. Kuningas, T. Rantanen, V. Haaslahti, T. Lövgren, *J. Fluoresc.* **2005**, *15*, 513–528.

Manuscript received: January 24, 2024  
Revised manuscript received: April 18, 2024  
Accepted manuscript online: April 22, 2024  
Version of record online: ■■■■■

## RESEARCH ARTICLE

Micro-RNAs are promising biomarkers, but better analytical methods are needed to enable their use in diagnostics. This article reports a simple hybridization assay for detection of micro-RNAs based on upconverting nanoparticle labels and stabilization of probe hybridization by DNA stacking, which is obtained by using hairpin structured probes.



*S. Kuusinen\*, S. Lahtinen, T. Soukka*

1 – 8

**Upconversion Luminescence Based Direct Hybridization Assay to Detect Subfemtomolar miR-20 a DNA Analogue in Plasma**

